

Material model for load rate sensitivity

Ivica Kožar^{*1a}, Adnan Ibrahimbegovic^{2a} and Tea Rukavina^{1,2b}

¹University of Rijeka Faculty of Civil Engineering, Radmile Matejčić 3, 51000 Rijeka, Croatia

²Sorbonne Universités / Université de Technologie Compiègne, Laboratoire Roberval de Mécanique
Centre de Recherche Royallieu, 60200 Compiègne, France

(Received June 7, 2017, Revised June 22, 2017, Accepted June 23, 2017)

Abstract. This work presents a novel model for analysis of the loading rate influence onto structure response. The model is based on the principles of nonlinear system dynamics, i.e., consists of a system of nonlinear differential equations. In contrast to classical linearized models, this one comprises mass and loading as integral parts of the model. Application of the Kelvin and the Maxwell material models relates the novel formulation to the existing material formulations. All the analysis is performed on a proprietary computer program based on Wolfram Mathematica. This work can be considered as an extended proof of concept for the application of the nonlinear solid model in material response to dynamic loading.

Keywords: lattice material model; nonlinear dynamical system; dynamic loading; Kelvin material model; Maxwell material model; sensitivity

1. Introduction

In this work, the structure is modeled as a nonlinear dynamical system. Typically, structures are modeled using the finite element method (FEM) and the material model is included into the continuum model, while discrete material models need some additional transformation to be included into FEM (e.g., see Marenčić and Ibrahimbegovic (2015) or Do *et al.* (2015a)). The approach adopted here formulates the structure model as a system of nonlinear differential algebraic equations with the material model integrated into it. As a result, the material model is directly coupled with the structure and there is a direct link between structure behavior and its parameters. Also, loading is a part of the structure description i.e. it is incorporated into differential equations describing the system, and one can determine the sensitivity to various material or loading parameters. This particular aspect is missing from the FEM model describing the nonlinear dynamical system. Advantages of solution of engineering problems by directly solving differential equations have also been recognized in Keivani *et al.* (2014).

Since loading is an integral part of the model, it is important to choose relevant representatives of the realistic loading. In our analysis, we are dealing with two types of loading: impact loading

*Corresponding author, Professor, E-mail: ivica.kozar@gradri.uniri.hr

^aProfessor, E-mail: adnan.ibrahimbegovic@utc.fr

^bPh.D. Student, E-mail: tea.rukavina@gradri.uniri.hr

characterized with the rate of application, and periodic loading characterized with the frequency.

The following section describes the impact and the periodic loading in detail, together with their derivatives and frequency characteristics, since it influences the model response. The third section describes the material model whose primary distinction from the classical approach is the introduction of the mass into the model. Damage based model with localization property in dynamic loading is also described in Do *et al.* (2015b). Differences in material behavior without and with the mass are also presented. Description of the material model ‘per se’ is meaningless in the model based on differential equations, so a two-cell structure is introduced as the simplest material model suitable for analysis. Two basic material types are analyzed: the nonlinear Kelvin and the nonlinear Maxwell material models, and some relevant material model properties are observed. The fourth section presents procedures and changes needed for investigation of larger structures. This is a basis for the development of a proprietary Mathematica program for the generation of the necessary nonlinear differential equations. An example of dynamic analysis of square lattice based on different approach can be found e.g., in Liu and Tang (2016). Finally, in the following section, some numerical examples are given, comparing the behavior of the Kelvin material and the Maxwell material-based models under the two types of loading.

2. Loading model

The Impulse loading alone would be used for determination of properties of a linear time invariant system, but since this is not our case, different loadings have to be applied. Sudden loading is simulated with the impact loading, but the periodic loading of different frequencies is also needed for the material response analysis. The amplitudes of the two types of loading are kept equal.

2.1 Impact loading

Impact loading is modeled with the logistic function for symmetric increase and decrease of the loading or the Gompertz cumulative distribution function for non-symmetry between increasing and decreasing loading parts. Displacement loading described as the logistic function and its derivative read

$$\varepsilon_a(t) = \frac{\varepsilon_0}{1 + \exp(-c(b + t))} ; \quad \varepsilon_a'(t) = \frac{c(\varepsilon_0 - \varepsilon_a(t))\varepsilon_a(t)}{\varepsilon_0} \quad (1)$$

Parameter ε_0 determines the amplitude, and parameter c determines the “steepness” of the curve, which corresponds to the load rate. In Fig. 1, there is loading and its derivative for constant b ($b = -2$) and c varying from 1 to 9, together with the phase plot of the loading.

One should notice that both the loading function and its derivative enter the system equations and that with the increase of the load rate (“steepness”) the derivative magnitude becomes larger.

Fourier analysis of the impact loading gives frequency content in a load applied on the structure and enables comparison of impact and periodic loading. Figs. 2-3 show the result of Fourier analysis of the loading and its derivative. It is important to notice that for certain parameter values there is a rich frequency content in the loading that is invisible without Fourier analysis.

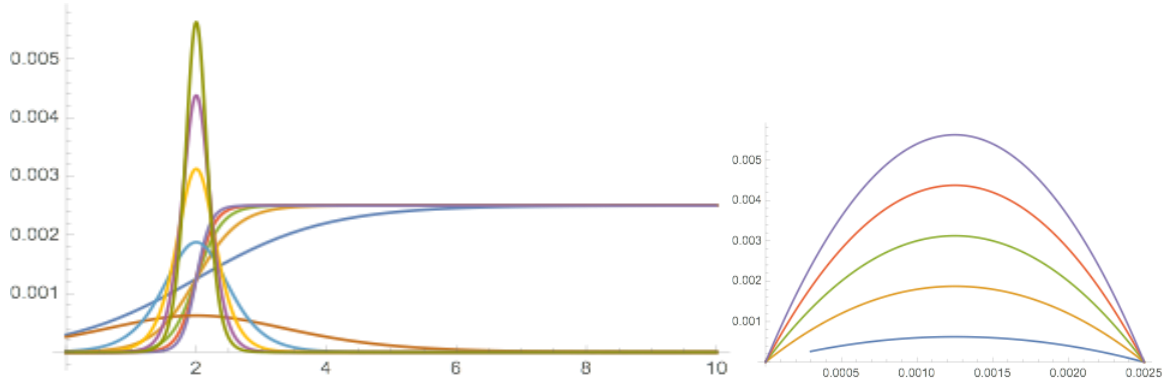


Fig. 1 Impact loading and its derivative, and phase plot for different load rates

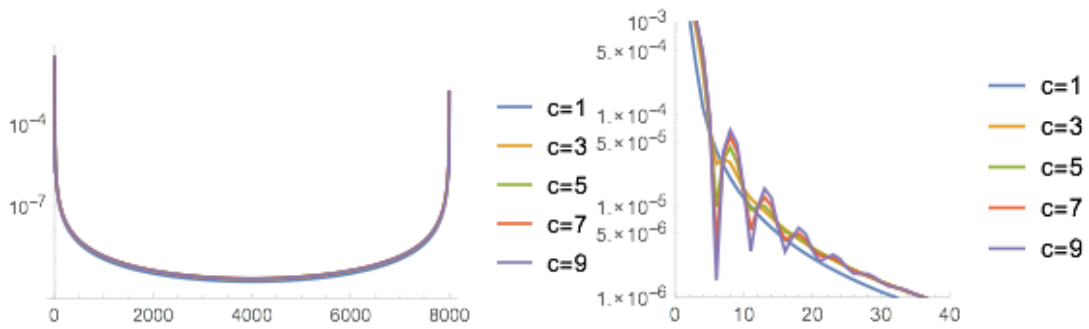


Fig. 2 Fourier analysis of impact loading for different load rates

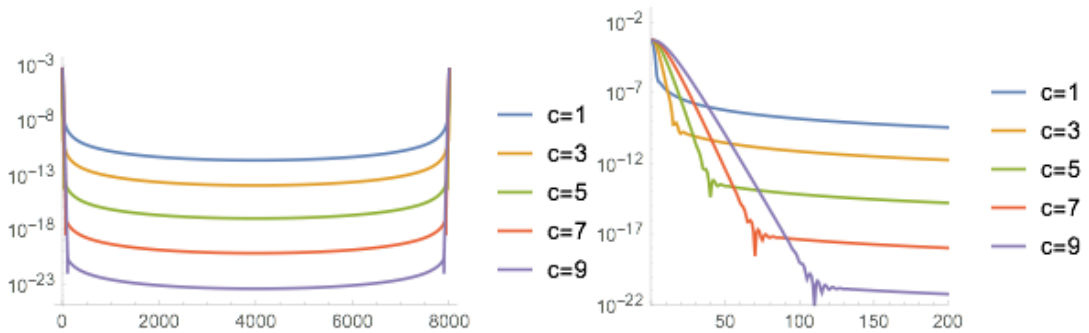


Fig. 3 Fourier analysis of the derivative of impact loading for different load rates

2.2 Periodic loading

Periodic loading is represented with harmonic functions of different frequencies and the same amplitude (ε_0) as the impact loading. In this case, we are using “chirp” function that has variable frequency

$$\varepsilon_a(t) = \varepsilon_0 \sin(2\pi t \cdot f(t))$$

$$\varepsilon_a'(t) = \varepsilon_0 \cdot 2\pi(f(t) + t \cdot f'(t)) \cos(2\pi t \cdot f(t)) \quad (2)$$

Function $f(t) = 0.05t + f_0$ with parameter f_0 determines the frequency of the loading. Note that the frequency is not constant. The amplitude of the loading is constant, but the amplitude of the derivative increases with time (time t enters the expression for amplitude). In addition, unlike with force loading, amplitude has to start from zero. Fig. 4 presents the periodic loading and its derivative for several frequency parameters f_0 . Fourier analysis of the periodic loading gives frequency content in a load applied on the structure. Figs. 5-6 show the result of Fourier analysis of the loading and its derivative.

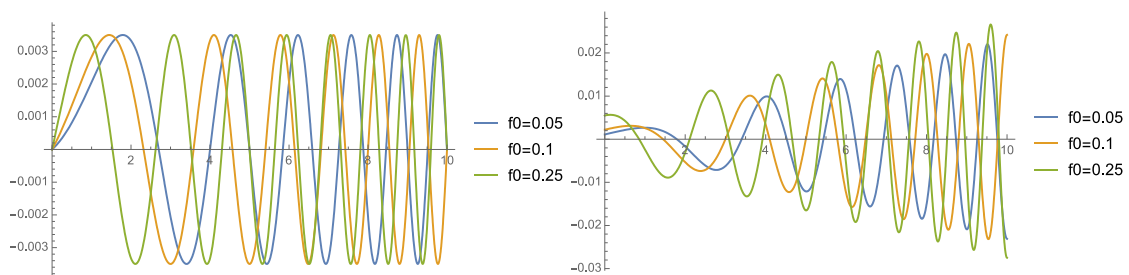


Fig. 4 Periodic loading and its derivative for different load frequencies

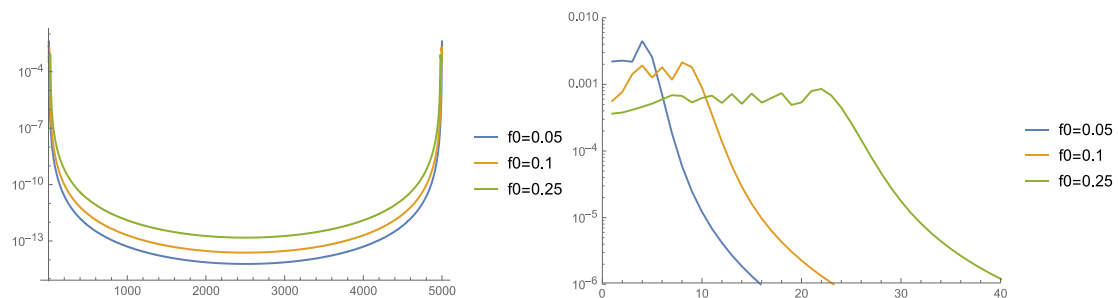


Fig. 5 Fourier analysis of periodic loading for different load frequencies

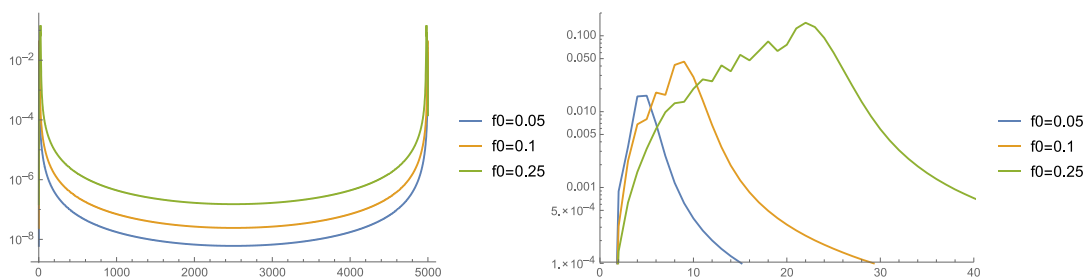


Fig. 6 Fourier analysis of the derivative of periodic loading for different load frequencies

3. Material model

Direct consequence of the loading type is the choice of the tool for structure response analysis, e.g., see Kantz and Schreiber (2003). In this work, the structure response is assessed using phase plots, spectrograms and PSD (power spectral density) plots. PSD is calculated as

$$E = \int_{-\infty}^{+\infty} |\hat{x}(f)|^2 df ; \hat{x}(f) = \int_{-\infty}^{+\infty} \exp(-2\pi ift) dt \quad (3)$$

In practical calculations, integrals are replaced with finite sums over frequencies f .

3.1 Nonlinear standard solid model

A material model is a nonlinear version of the standard solid model (see Simo and Hughes 1998, Ibrahimbegovic 2009) that is a combination of basic Maxwell and Kelvin material models in a way that with a suitable choice of material parameters it is possible to obtain either one of the basic models, or some combination of them. One could say that the basic models are the two limits and the model behavior lays somewhere between those two extremes.

Equations of the non-linear standard solid model

$$\begin{aligned} e(t) &= e_{Kalman}(t) = e_{elastic}(t) + e_{viscous}(t) \\ S(t) &= S_{elastic}(t) + S_{Maxwell}(t) \\ S_{elastic}(t) &= e_{Kalman}(t) \times E(e_{Kalman}(t)) \\ S_{Maxwell}(t) &= e_{elastic}(t) \times E(e_{elastic}(t)) = m \frac{e_{viscous}(t)}{t} \end{aligned} \quad (4)$$

where either $\varepsilon_{elastic}$ or $\varepsilon_{viscous}$ could be chosen as internal model variables. Limits of Kalman modulus of elasticity ($E_{Kalman} = E(\varepsilon_{Kalman}) = 0$) or Maxwell modulus of elasticity ($E_{Maxwell} = E(\varepsilon_{elastic}) = 0$) in the standard solid model restore the Maxwell or the Kelvin material model.

The behavior of the internal variable is very important for the material model; some comparison could be driven from the viscoelastic model. The evolution equation of the internal variable for linear viscoelasticity model is

$$\sigma = E_1(\theta)\zeta + \varepsilon_v(\theta)\dot{\zeta} \rightarrow \dot{\zeta} = -\frac{E_1(\theta)}{\varepsilon_v(\theta)}\zeta + \frac{1}{\varepsilon_v(\theta)}\sigma =: f(\sigma, \theta, \zeta) \quad (5)$$

Analytic solution of this differential equation is taken from Ibrahimbegovic (2009)

$$\zeta(t) = \zeta(0) \exp(-t/\tau) + \int_0^t \frac{1}{\varepsilon_v(\theta)} \exp[-(t-s)/\tau] \sigma(s) ds ; \tau = \frac{\varepsilon_v}{E_1} \quad (6)$$

The parameter $\tau = \varepsilon_v(\theta) / E_1(\theta)$ is called the characteristic time of the standard viscoelasticity model, capturing the rate of evolution of internal variables with respect to a variation of the stress imposed by a particular loading. This shows that the scale of evolution of internal variable $\varepsilon_{viscous}$ should be much faster than the time scale of other state variables. If, however, the viscosity component of the model is combined with the mass effect, the inertia 'component' of the model interferes with the difference between higher vs. lower rate of loading.

Nonlinear behavior of the elastic modulus $E(\varepsilon(t)) = w(\varepsilon(t))E_0 = \varepsilon(t) \exp(-\varepsilon(t)/a)$ is taken from the microplane material model (see Kožar and Ožbolt 2010); E_0 is the initial modulus of elasticity. The exponential softening behavior of the modulus of elasticity can be obtained from homogenization of the fiber bundle model (e.g. see Kun *et al.* 2007). The nonlinear characteristic

of the elastic modulus has a great influence on the system behavior.

In structure models based on differential algebraic equations, it does not make sense to analyze a material model as a single cell, instead two cell models are used for determination of the influence of various parameters, see Fig. 7.



Fig. 7 Kelvin and Maxwell material models as an assembly of two cells

Material models in Fig. 7 are connected without any mass in nodes; however, there could be mass in nodes resulting in different systems of differential equations (e.g., a system of differential algebraic equations (DAE) turns into a system of ordinary differential equations (ODE)).

Detailed description of the two cells Maxwell model under impact loading can be found in Kožar and Ožbolt (2010) and of the two cells Kelvin model in Kožar *et al.* (2012). Here we add spectral analysis and parameter sensitivity.

3.2 Massless solid model

The system of DAE for the massless model consisting of two connected cells takes different forms for Kelvin and Maxwell model types:

- Differential equation for the Kelvin model

$$\frac{d}{dt} \varepsilon_1(t) = \frac{1}{\mu_1 + \mu_2} \left[E_2 \cdot w(\varepsilon_a(t) - \varepsilon_1(t)) - E_1 \cdot w(\varepsilon_1(t)) + \mu_2 \frac{d}{dt} \varepsilon_a(t) \right] \quad (7)$$

where function $\varepsilon_a(t)$ is the loading.

- System of three differential-algebraic equations for the Maxwell model

$$\begin{aligned} \frac{d}{dt} e_{v1}(t) &= f_1(x_1(t), e_{v1}(t)) \\ \frac{d}{dt} e_{v2}(t) &= f_2(x_1(t), e_{v2}(t), e_a(t)) \\ m_{01} \times f_1(x_1(t), e_{v1}(t)) - m_{02} \times f_2(x_1(t), e_{v2}(t), e_a(t)) &= 0 \end{aligned} \quad (8)$$

where functions f_1 and f_2 are

$$\begin{aligned} f_1(x_1(t), e_{v1}(t)) &= \left(\frac{x_1(t)}{L_1} - \varepsilon_{v1}(t) \right) \frac{E_{01}}{\mu_{01}} \exp\left(\frac{\varepsilon_{v1}(t)}{a} - \frac{x_1(t)}{aL_1} \right) \\ f_2(x_1(t), e_{v1}(t)) &= \left(\frac{x_1(t)}{L_1} - \varepsilon_{v1}(t) \right) \frac{E_{01}}{\mu_{01}} \exp\left(\frac{\varepsilon_{v1}(t)}{a} - \frac{x_1(t)}{aL_1} \right) \end{aligned} \quad (9)$$

and a is the loading parameter.

In the Maxwell equilibrium equation x_1 is the displacement of the midpoint between the two material cells.

In the previous work, Kožar and Ožbolt (2010), the third of Eq. (8) was different because algebraic condition had to be manually included into the system of differential equations and Radau integration procedure was needed to obtain localization. Now, owing to the use of Wolfram Mathematica (2017), the integration algorithm applies automatic switching and this simpler algebraic condition can be used. Moreover, the previous formulation of Eq. (8) did not allow for the generalization of the equation assembly procedure; now, Eqs. (4), (7) and (8) could be successfully generalized into the system of differential equations described later.

Equilibrium equations describe stress equilibrium inside the model; for the Kelvin model it is incorporated into Eq. (7), and for the Maxwell model it is the third equation in Eq. (8).

Equilibrium equations for the presented models exhibit the bifurcation possibility, without any artificial enforcing of the localization. Bifurcation is interesting phenomena observed in many materials as is seen e.g., in Toh *et al.* (2016). The numerical integration algorithm and time step size are important for localization; for some parameter values solutions are close and switching between solution paths is possible. Fig. 8(a) shows solutions of differential Eq. (7) (Kelvin model) and Eq. (8) (Maxwell model). Actually, solutions of Eq. (8) are midpoint displacement $x_1(t)$ and viscous deformations $\varepsilon_{v1}(t)$ and $\varepsilon_{v2}(t)$. In order to obtain compatibility of solutions, Fig. 8(a) shows the elastic part of the deformation

$$e_{e1}(t) = x_1(t) - e_{v1}(t), e_{e2}(t) = e_a(t) - x_1(t) - e_{v1}(t) \quad (10)$$

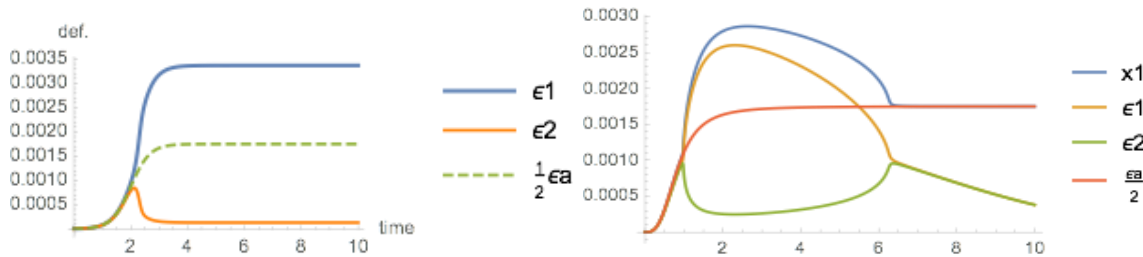


Fig. 8(a) Kelvin and Maxwell model solutions in time

The influence of material parameters can be assessed using sensitivity analysis but it is loading dependent and has to be performed separately for the impact and for the periodic loading. It is possible to observe the behavior of the equilibrium equation in Fig. 8 as one changes the elasticity parameter E and viscosity parameter μ . Even more interesting is to observe changes in the solutions of differential equations as parameter change. Two approaches are possible: i) one could parameterize the numerical solutions or ii) one could calculate the partial derivative of the solution with respect to the desired parameter. One should note that i) is a prerequisite for ii). The parametric numerical solution could be obtained with careful data manipulation of the so-called “unresolved parameters”. The idea is to keep parameters as symbols during numerical manipulations and determine their numeric value later; in Wolfram Mathematica (2017) that is done automatically. Note that parameters get into the solution of the differential equation (or the solution of the system of differential and algebraic equations).

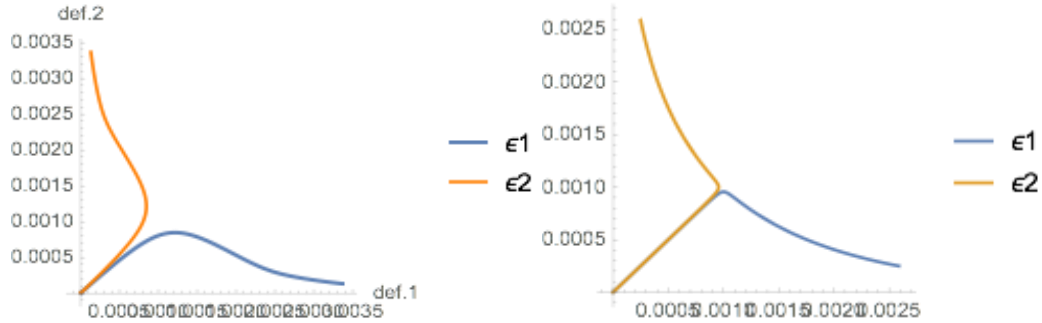


Fig. 8(b) Kelvin and Maxwell model solutions in parametric space (ϵ_{e1} vs. ϵ_{e2})

3.2.1 Impact loading

It is important to note that the impact-loading derivative is included into the solution of the differential equation (that it is the reason for presenting it in Figs. 1-3).

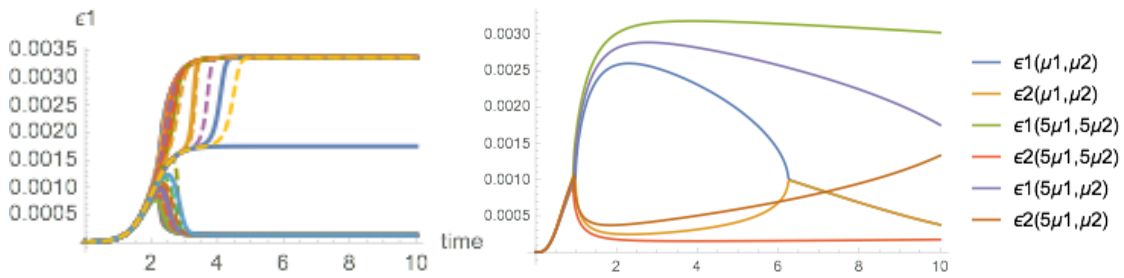


Fig. 9(a) Kelvin and Maxwell, viscosity parameter sensitivity in time

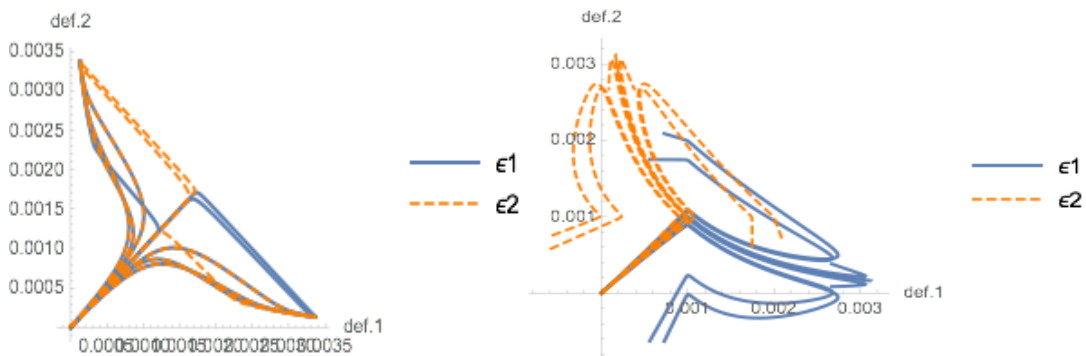


Fig. 9(b) Kelvin and Maxwell, viscosity parameter sensitivity in parametric space (ϵ_{e1} vs. ϵ_{e2})

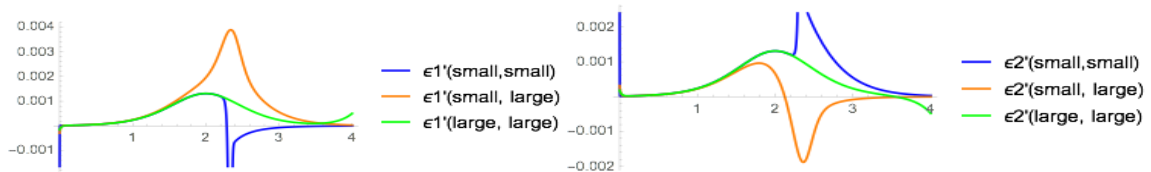


Fig. 9(c) Kelvin, rate of deformation sensitivity in time

Results of the sensitivity analysis in the time domain and in the parameter space are presented in Figs. 9(a)-(b). We can see the domain the solution is spanned as viscosity parameters change; also, the viscosity parameter value influences the starting time of bifurcation.

The rate of deformation is directly proportional to the stress so that sensitivity is of importance and is depicted in Fig. 9(c) as a function of the two viscosity parameters (μ_1, μ_2).

There is no strain rate evaluation for the Maxwell model since stress is a sum of elastic and viscous parts. Instead, there is stress evaluation in the model with added mass.

Fig. 10 presents a phase plot of the Kelvin model for one large and one small viscosity parameter, and with localization clearly visible.

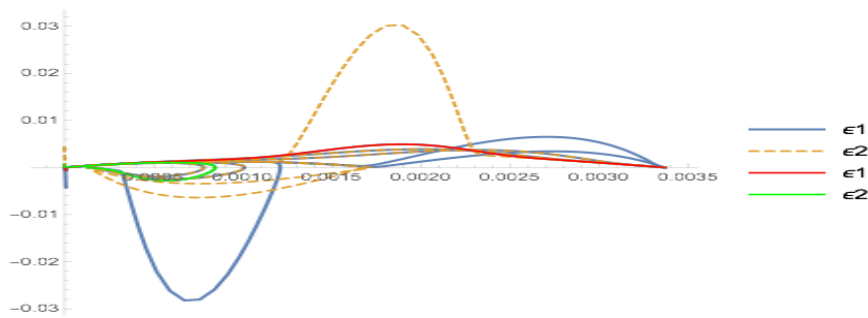


Fig. 10 Kelvin, phase plot for one large and one small viscosity parameter

3.2.2 Periodic loading

For periodic loading, it is possible to obtain a spectrogram and see the material behavior dependent on the loading frequency. Numerical experiments have been performed for periodic loading described above and typical results are presented in the following figures.

Results of the sensitivity analysis in the time domain and in the parameter space are presented in Fig. 11(a)-(b). We can see the domain the solution is spanned as viscosity parameters change; also, the viscosity parameter value influences the starting time of bifurcation.

The rate of deformation is directly proportional to the stress so that sensitivity is of importance and is depicted in Fig. 11(d) as a function of the two viscosity parameters (μ_1, μ_2).

Fig. 12 presents a phase plot of the Kelvin model for one large and one small viscosity parameter; for periodic loading, localization is periodic, too.

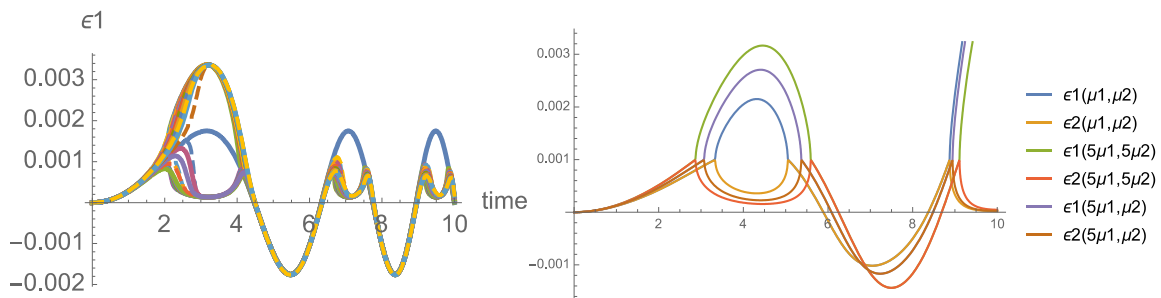


Fig. 11(a) Kelvin and Maxwell, viscosity parameter sensitivity in time

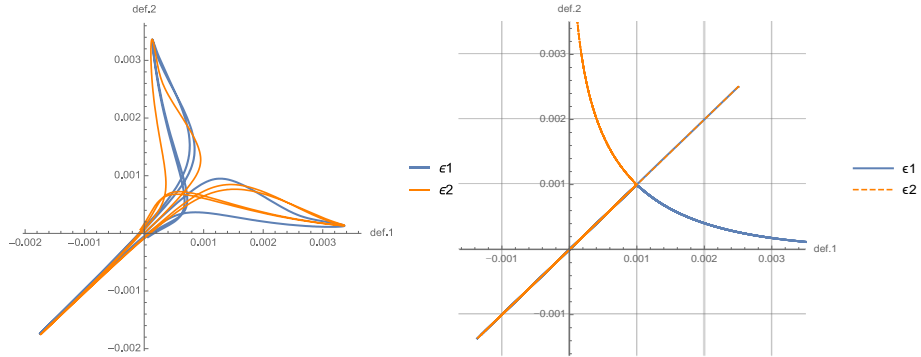


Fig. 11(b) Kelvin and Maxwell, viscosity parameter sensitivity in parametric space (ϵ_{e1} vs. ϵ_{e2})

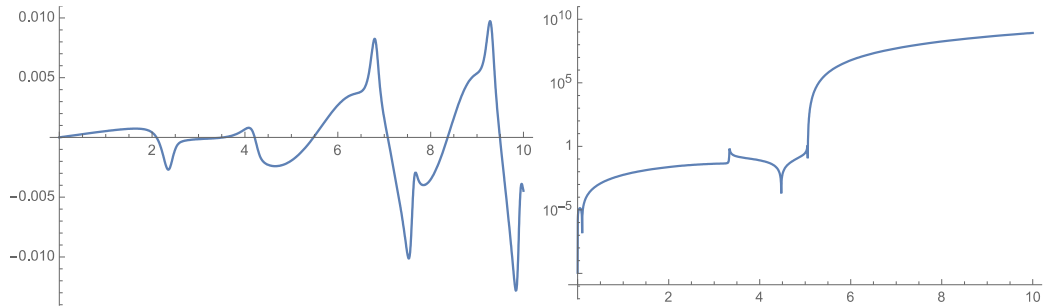


Fig. 11(c) Kelvin, Maxwell, rate of deformation sensitivity in time

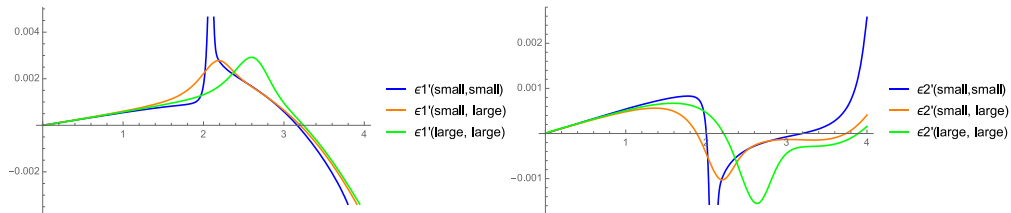


Fig. 11(d) Kelvin, rate of deformation sensitivity in time

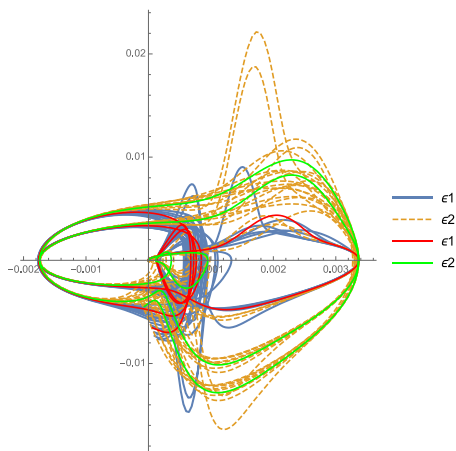


Fig. 12 Kelvin, phase plot for one large and one small viscosity parameter

3.3 Solid model with mass

In standard FEM models, mass is a structural property and is not part of the material model. Inspection of basic properties of massless models shows that they are capable of localization and fracture modeling within a material. Consequently, it is tempting to formulate the material model without a mass that can be added later at the structural level. However, comparison of massless models versus those with a mass show that mass is important in material parameter determination and in realistic modeling of loading rate dependency.

In our model based on DAE, mass has to be included into the material model. Consequently, the system of DAE for Maxwell model transforms into a system of ODE and Eq. (8) has to be rewritten.

The Kelvin Eq. (7) becomes a system of ODE

$$\frac{d}{dt}\zeta_1(t) = \frac{1}{m} \left[E_2 w(\varepsilon_a(t) - \varepsilon_1(t)) - E_1 w(\varepsilon_1(t)) + \mu_2 \frac{d}{dt} \varepsilon_a(t) - (\mu_1 + \mu_2) \zeta_1(t) \right] \quad (11)$$

From Eq. (11) sensitivity equations could be derived as derivatives over parameters but only after all functions are modified so that the corresponding parameters get exposed, e.g., $\varepsilon_q(t)$ becomes $\varepsilon_q(t, m)$ for assessing mass sensitivity, etc.

$$Sens_m = \frac{\partial \varepsilon_1(t)}{\partial m}, Sens_{\mu_1} = \frac{\partial \varepsilon_1(t)}{\partial \mu_1}, Sens_{\mu_2} = \frac{\partial \varepsilon_1(t)}{\partial \mu_2}, Sens_{\delta} = \frac{\partial \varepsilon_1(t)}{\partial \delta} \quad (12)$$

The Maxwell model DAE equations turn into a system of ODE

$$\begin{aligned} \frac{d}{dt} e_{v1}(t) &= f_1(x_1(t), e_{v1}(t)) \\ \frac{d}{dt} e_{v2}(t) &= f_2(x_1(t), e_{v2}(t), e_a(t)) \\ m_1 \frac{d^2 x_1(t)}{dt^2} &= m_{01} \times f_1(x_1(t), e_{v1}(t)) - m_{02} \times f_2(x_1(t), e_{v2}(t), e_a(t)) \end{aligned} \quad (13)$$

Parameter sensitivity equations for Maxwell model are (derivatives are over parameters)

$$\begin{aligned} Sens_m &= \frac{\partial \varepsilon_{v1}(t)}{\partial m}, Sens_{\mu_1} = \frac{\partial \varepsilon_{v1}(t)}{\partial \mu_1}, Sens_{\mu_2} = \frac{\partial \varepsilon_{v1}(t)}{\partial \mu_2}, Sens_{\delta} = \frac{\partial \varepsilon_{v1}(t)}{\partial \delta} \\ Sens_m &= \frac{\partial \varepsilon_{v2}(t)}{\partial m}, Sens_{\mu_1} = \frac{\partial \varepsilon_{v2}(t)}{\partial \mu_1}, Sens_{\mu_2} = \frac{\partial \varepsilon_{v2}(t)}{\partial \mu_2}, Sens_{\delta} = \frac{\partial \varepsilon_{v2}(t)}{\partial \delta} \\ Sens_m &= \frac{\partial x_1(t)}{\partial m}, Sens_{\mu_1} = \frac{\partial x_1(t)}{\partial \mu_1}, Sens_{\mu_2} = \frac{\partial x_1(t)}{\partial \mu_2}, Sens_{\delta} = \frac{\partial x_1(t)}{\partial \delta} \end{aligned} \quad (14)$$

Functions in Maxwell model need to simultaneously expose much more parameters in order to enable sensitivity analysis, e.g., $f_1(x_1(t), \varepsilon_{v1}(t))$ turns into $f_1(x_1(t), \varepsilon_{v1}(t), m, \mu_1, \mu_2, \delta)$. Besides calculating sensitivity equations that are difficult in more complicated realistic cases, it is possible to perform parametric analysis, i.e., solve a resulting system of differential equations for different parameter values, which is often done.

3.3.1 Impact loading

Solution for impact loading for the mass model is similar to the massless model for a small mass. However, there is an interesting solution when a hidden dynamic component in impact loading excites the model; vibrations are visible from the very beginning of the loading and they are even more visible in the rate of deformation. Fig. 13(a) depicts the vibrating solution; Fig. 13(b) is the same in parametric (ε_1 vs. ε_2) and phase space. Fig. 13(c) presents stresses σ_1, σ_2 in time and in parametric space (σ vs. ε). Stresses in parametric space are multiplied with a small value that changes in time in order to make the stress path visible; normally, stresses change along the same path and then change is not visible.

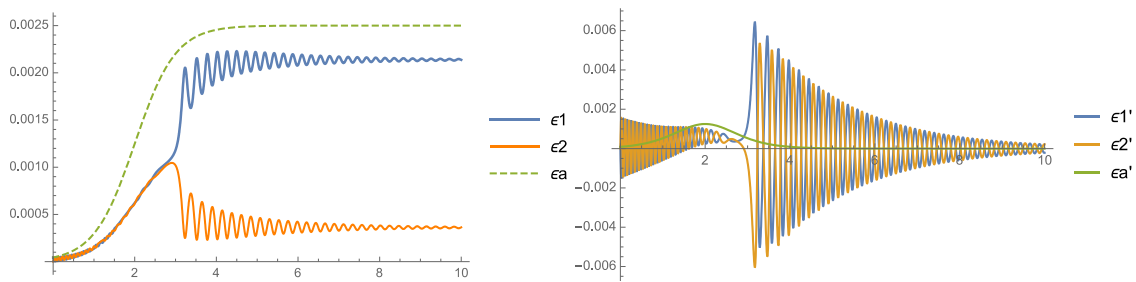


Fig. 13(a) Kelvin, deformation and its derivative in time

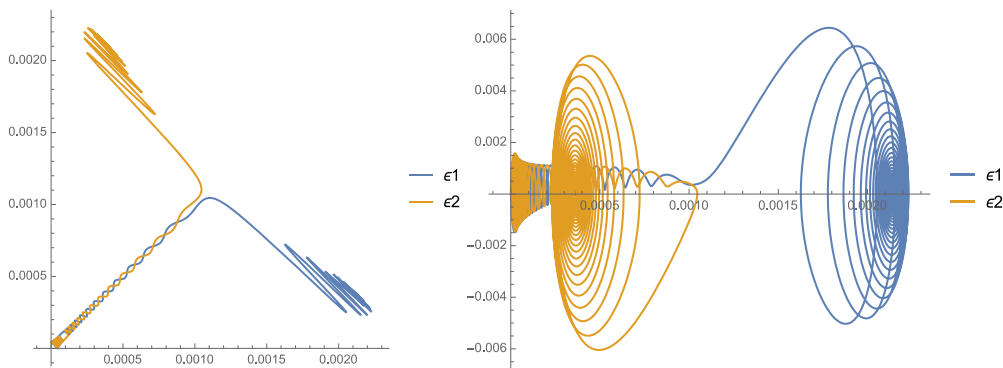


Fig. 13(b) Kelvin, deformations in parametric space (ε_{e1} vs. ε_{e2})

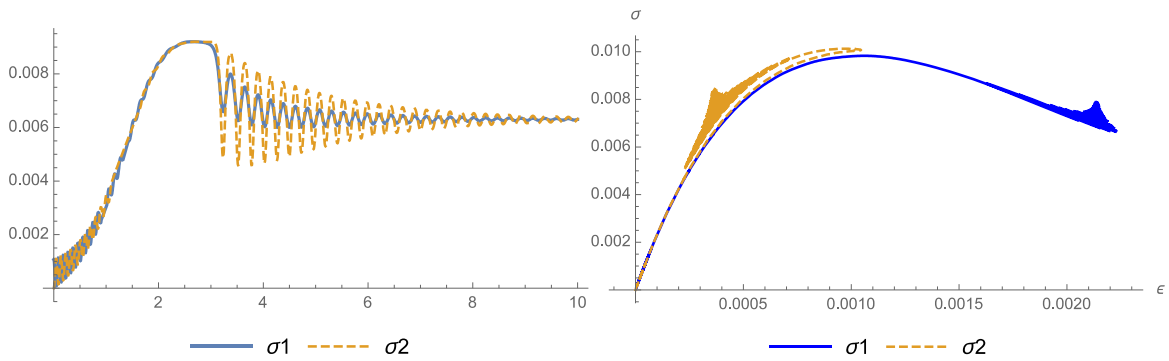


Fig. 13(c) Kelvin, stress in time and in parametric space (σ vs. ε)

Introduction of a mass into the Maxwell model enforces localization even in completely symmetric cases. In Figs. 14 the behavior of the Maxwell model is depicted under impact loading. As in the Kelvin model, stresses in parametric space are multiplied with a small value. Comparing the stresses with the Kelvin model, we see that there is initial stress oscillation around the opposite sides of the stress peak, and after that both stresses recover and approach the peak value; if a different unloading path would be introduced, that would not be possible.

From sensitivity analysis in Fig. 15 we see that the Maxwell model is not particularly sensitive neither to load rate nor to mass changes. In addition, sensitivity on mass change is much greater than sensitivity on load rate change.

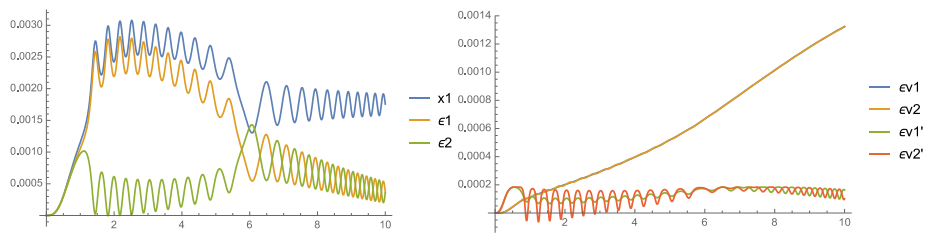


Fig. 14(a) Maxwell, elastic and viscous deformations (and derivatives) in time

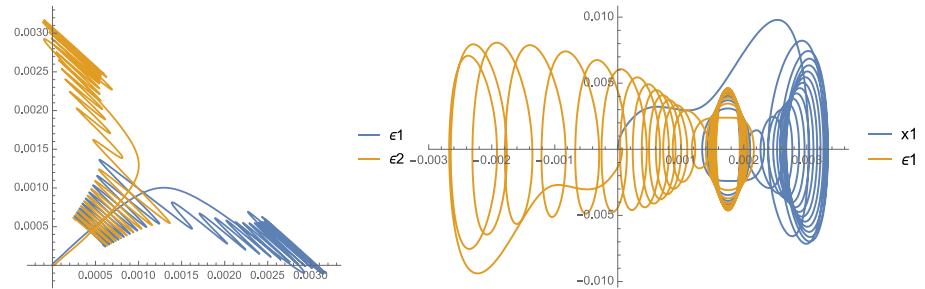


Fig. 14(b) Maxwell, deformations in parametric space (ϵ_{e1} vs. ϵ_{e2})

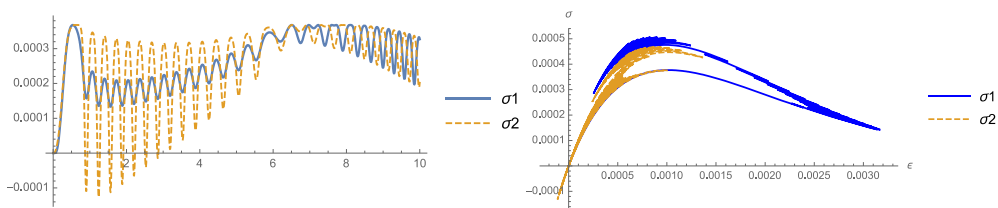


Fig. 14(c) Maxwell, stress in time and in parametric space (σ vs. ϵ)

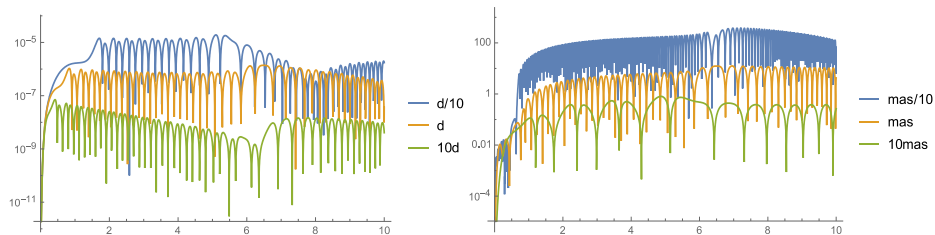


Fig. 15 Maxwell, sensitivity on load rate and mass

3.3.2 Periodic loading

For models with mass, periodic loading has been somewhat changed from the one presented in Fig. 4. The loading is now tension only, as presented in Fig. 16.

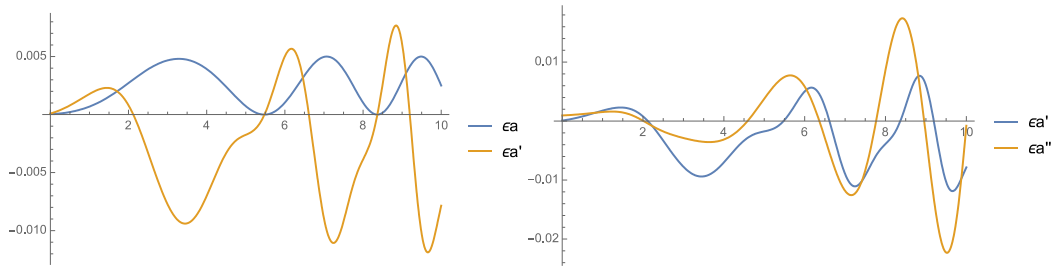


Fig. 16 Periodic loading whole in tension, and its first and second derivatives

Fig. 16 shows that although the loading is in tension only, its derivatives change sign and grow constantly.

The behavior of the Kelvin model with small mass ($m = 0.01$) under periodic all tension loading (as depicted in Fig. 16) is presented in Fig. 17.

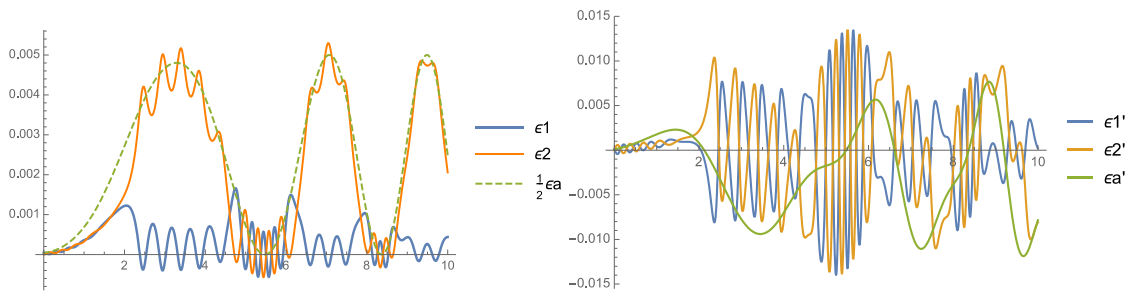


Fig. 17(a) Kelvin, deformations and its derivative in time

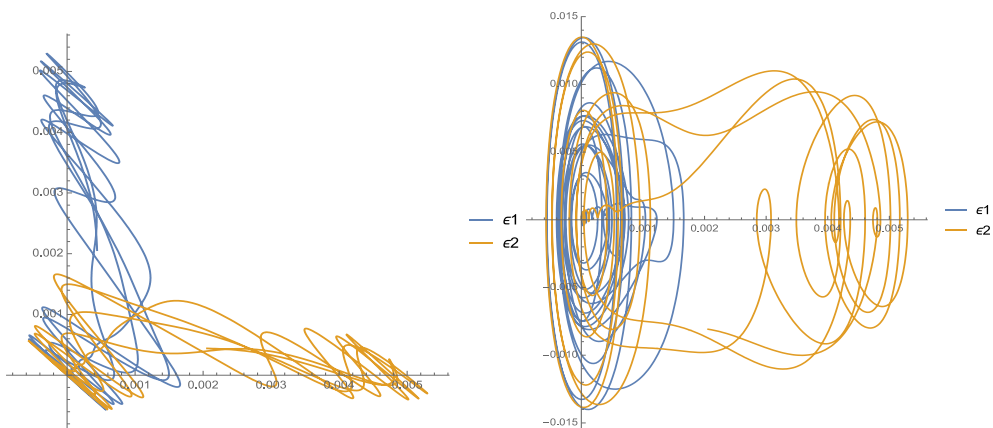


Fig. 17(b) Kelvin, deformations in parametric space (ϵ_{e1} vs. ϵ_{e2})

Figs. 18 present the stress change in the model instead of the mass sensitivity analysis. From comparison of stresses in models without and with the mass, it is evident that the model with the mass loaded entirely in tension, is compression dominated (in this case when the model does not break in tension).

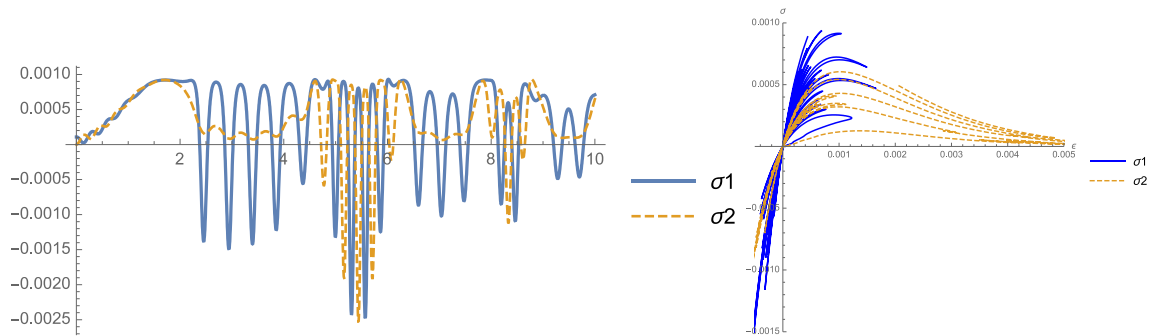


Fig. 18(a) Kelvin, $m = 0.01$ stress in time and in parametric space (σ vs. ϵ)

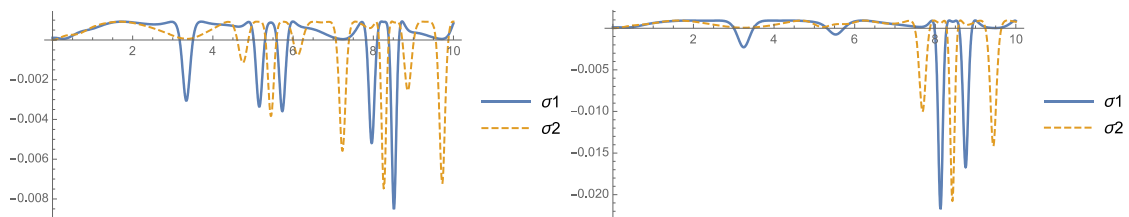


Fig. 18(b) Kelvin, $m = 0.05$ stress in time and $m = 0.1$ stress in time

With the increasing mass, the domination of the compressive stresses grows; also, large mass delays the appearance of large compressive stresses, i.e., for a larger mass, tension periodic loading must last longer in order for compressive stresses to appear.

4. Structure models

Structure models comprise a greater number of material cells limited only by computer capacity. Accordingly, one has to devise methods for automatic generation of DAE. Matrix formulation is adopted in this work, taking into account different properties of Maxwell and Kelvin models. The formulation resembles classical formulation in structure analysis to ease comparison of results although the presented model retains the form of a system of nonlinear differential (algebraic) equations. It is done to preserve generality of the model since, although the present material model with nonlinear exponential spring and constant viscosity could be transformed into a system of nonlinear algebraic equations, it will not be the case in the future, where we plan to combine different material models and cyclic material behavior.

The structure is analyzed as an assembly of elementary lattices (bars) where the assembly process is the same as in the finite element method so the final matrix equations resemble the finite element method formulation (note that the resulting matrix equations are nonlinear and the only

constant matrix is the mass matrix). Equations for Kelvin and Maxwell are, respectively (time dependency of all the variables is assumed and is not written explicitly)

$$\begin{aligned} \mathbf{M}\ddot{\mathbf{x}} + \mathbf{C}_K(\mathbf{x}, \dot{\mathbf{x}}) + \mathbf{K}_K(\mathbf{x}) &= \mathbf{F}(t) \\ \mathbf{x} &= \boldsymbol{\varepsilon}_e = \boldsymbol{\varepsilon}_v \end{aligned} \quad (15)$$

$$\begin{aligned} \mathbf{M}\ddot{\mathbf{x}} + \mathbf{K}_M(\mathbf{x}) &= \mathbf{F}(t) \\ \mathbf{C}_M(\dot{\boldsymbol{\varepsilon}}_v) &= \mathbf{K}_M(\boldsymbol{\varepsilon}_e) \\ \mathbf{x} &= \boldsymbol{\varepsilon}_e + \boldsymbol{\varepsilon}_v \end{aligned} \quad (16)$$

\mathbf{M} , \mathbf{C}_K , \mathbf{K}_K are mass, damping and stiffness matrices for Kelvin (K) or Maxwell (M) model, respectively. $\boldsymbol{\varepsilon}_e$, $\boldsymbol{\varepsilon}_v$ are elastic and viscous components of displacement (or their time derivatives when with ‘dot’).

Maxwell model is much more demanding since it comprises internal variable vector $\boldsymbol{\varepsilon}_v(t)$. The consequence is an additional system of equations describing the internal variable behavior. Loading can be expressed with time dependent force $F_i(t)$ or with time dependent displacement $x_i(t)$ or time dependent boundary conditions or a combination of both; for a more elaborate description of the difference see Kožar and Ožbolt (2010).

Solution of the systems of nonlinear differential Eqs. (15)-(16) has been performed in Wolfram Mathematica (2017) but some other solver could be used as well (e.g., XPPAUT 8.0 from 2016, for instructions the only available written source is Ermentrout 2002). Some solvers cannot deal with derivatives higher than one, in which case each second order equilibrium equation (with \ddot{x}) is easily transformed into two first order differential equations (which brings additional ‘ n ’ equations into the system). This procedure is not necessary in Mathematica and it is increasingly used in engineering calculations (e.g., see Ziaolhagh *et al.* 2016).

Note: there are ‘ n ’ (n = number of nodes) kinematic equations and ‘ n ’ equilibrium equations (or $2n$ for a system expressed in normal form) but ‘ m ’ (m = number of lattices) compatibility equations.

Stiffness and damping expanded matrix formulation with included functions describing the Kelvin lattice reads

$$\begin{aligned} k^{eK}[x] &= \begin{pmatrix} f_i(x_i, x_j) \\ f_j(x_i, x_j) \end{pmatrix} = EA^e \cdot \begin{pmatrix} 1 \\ -1 \end{pmatrix} \cdot w \left(\mathbf{B} \cdot \begin{pmatrix} x_i \\ x_j \end{pmatrix} \right) \\ c^{eK}[x] &= \begin{pmatrix} \mu_i(x_i, x_j) \\ \mu_j(x_i, x_j) \end{pmatrix} = \mu^e \cdot \left(\mathbf{B} \cdot \begin{pmatrix} \dot{x}_i \\ \dot{x}_j \end{pmatrix} \right) \end{aligned} \quad (17)$$

Stiffness and damping expanded matrix formulation with included functions describing the Maxwell lattice reads

$$\begin{aligned} k^{eM}[x - \boldsymbol{\varepsilon}_v] &= \begin{pmatrix} f_i(x_i, x_j, \boldsymbol{\varepsilon}_v) \\ f_j(x_i, x_j, \boldsymbol{\varepsilon}_v) \end{pmatrix} = EA^e \cdot \begin{pmatrix} 1 \\ -1 \end{pmatrix} \cdot w \left(\mathbf{B} \cdot \begin{pmatrix} x_i \\ x_j \end{pmatrix} - \boldsymbol{\varepsilon}_v^e \right) \\ c^{eM}[\boldsymbol{\varepsilon}_v] &= \begin{pmatrix} \mu_i(x_i, x_j, \boldsymbol{\varepsilon}_v) \\ \mu_j(x_i, x_j, \boldsymbol{\varepsilon}_v) \end{pmatrix} = \mu^e \cdot \left(\mathbf{B} \cdot \begin{pmatrix} \dot{x}_i \\ \dot{x}_j \end{pmatrix} - \boldsymbol{\varepsilon}_v \right) \end{aligned} \quad (18)$$

In both equations, $w(\dots)$ is a function of spring behavior and matrix \mathbf{B} is displacement-strain transformation, so $\boldsymbol{\varepsilon} = \mathbf{B}\mathbf{x}$. Programming the automatic assembly of the above formulation is performed in Wolfram Mathematica (2017). Structures based on the standard model are a

combination of these two types of cells.

5. Numerical examples

The discretization of the structure model is based on Hrennikoff as presented in van Mier (2013). Hrennikoff model discretizes a rectangle with six bars (two vertical, two horizontal, two diagonal) whose area is determined from $A_{hor} = db/2 (9 - 3\alpha^2)/8$, $A_{ver} = da/2 (9 - 3\beta^2)/8$, $A_{diag} = dl/2 \sqrt{3}/8 (\alpha + \beta)$; a, b, d are rectangle length, height and thickness respectively and $\alpha = a/b$, $\beta = b/a$, $l = \sqrt{a^2 + b^2}$. The presented bar dimensions ensure the same behavior in the elastic regime as in the theory of elasticity. Rectangle dimensions are 10 by 10 units with thickness 0.1 units. The structure is simply supported in the bottom and the top line of nodes and displacement loading is applied in node 23.

The structure model to be analyzed is presented in Fig. 19, with node numbers and some cell numbers; each cell is represented as a bar and comprises either the Kelvin or the Maxwell nonlinear model, and there is an equal mass in every node. In Wolfram Mathematica, such a structure is treated as a network described with the network incidence matrix and the connecting cells are represented with arrows or bars.

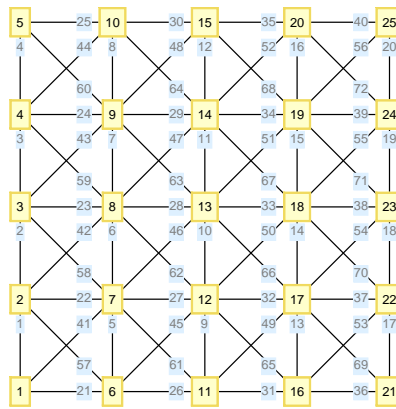


Fig. 19 Kelvin and Maxwell structure models for analysis

The model is completely symmetric (no localization initiators, they are not necessary for models based on nonlinear system dynamics) and data is: a) for the Kelvin model $E_0 = 2.5$, $\mu_0 = 0.00125$, $m_0 = 0.1$, b) for the Maxwell model $E_0 = 1.0$, $\mu_0 = 2.0$, $m_0 = 0.003$.

The Kelvin model comprises of 50 second order nonlinear differential equations and the Maxwell model of 122 second order nonlinear differential equations. All the equations and the corresponding initial conditions were automatically produced by a proprietary Mathematica program and solved afterwards in 5 to 12 seconds. The produced system of nonlinear differential equations and the initial conditions can be exported to any solver or program for solution and processing.

5.1 Impact loading

The loading is the same as presented in Fig. 1 but with opposite sign and different rates, and is applied in node 23; the displacement results for the two models are visible in Figs. 20. From the Kelvin model in Fig. 20(a) it is visible that impact on one side causes eruption of the material on the other. The strain wave for slow loading activates a larger area of the specimen and the wave propagation is slower. Faster loading is much more concentrated and strain wave propagation is much faster.

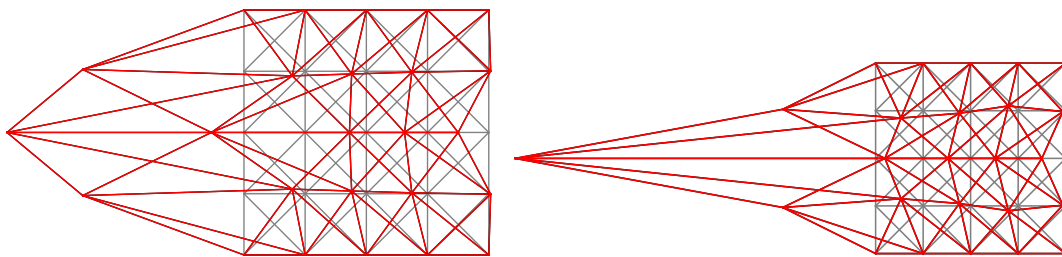


Fig. 20(a) Kelvin structure under slow and fast impact, after $t=20$ and $t=4$ time units

In the Maxwell model, there is no eruption of the material, it behaves like fluid and impact on one side only causes waves on the other; load rate makes no difference. Variation of material parameters describes different fluid behavior, from light to sticky. The Maxwell model is depicted in Fig. 20(b) for fast loading and three different instances of time.

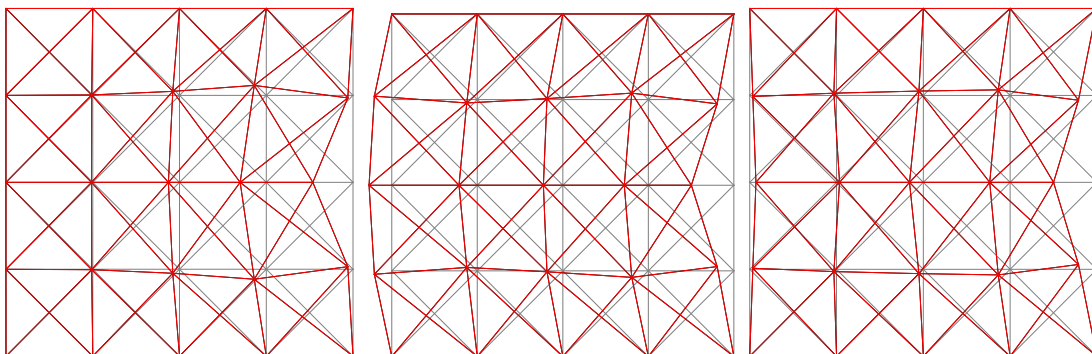


Fig. 20(b) Maxwell structure under fast impact, after $t=0.8$, $t=1.8$ and $t=3.3$ time units

5.2 Periodic loading

Periodic loading is as presented in Fig. 4 with prolonged analysis time to $T=20$ time units and material parameters are as presented in two cell examples.

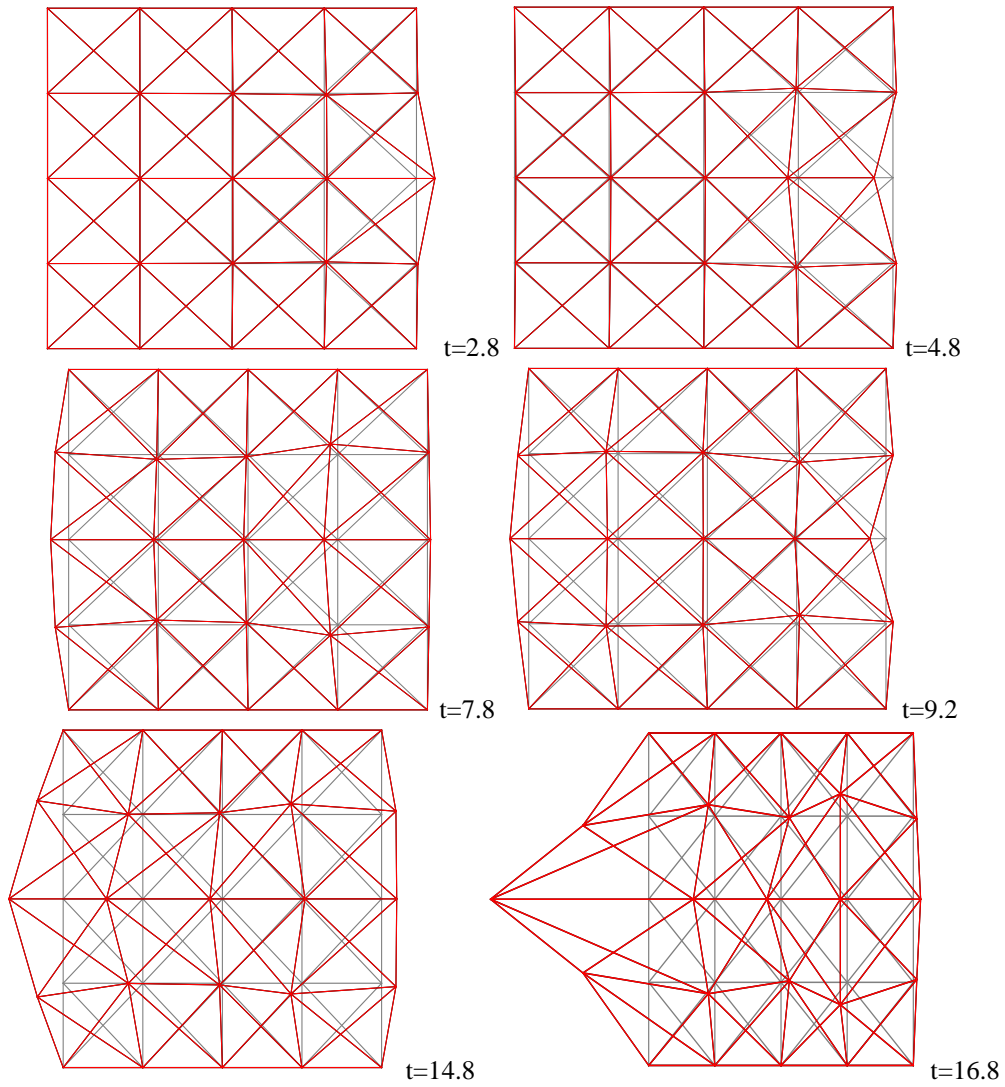


Fig. 21(a) Kelvin structure models in times $t = 2.8, 4.8, 7.8, 9.2, 14.8, 16.8$

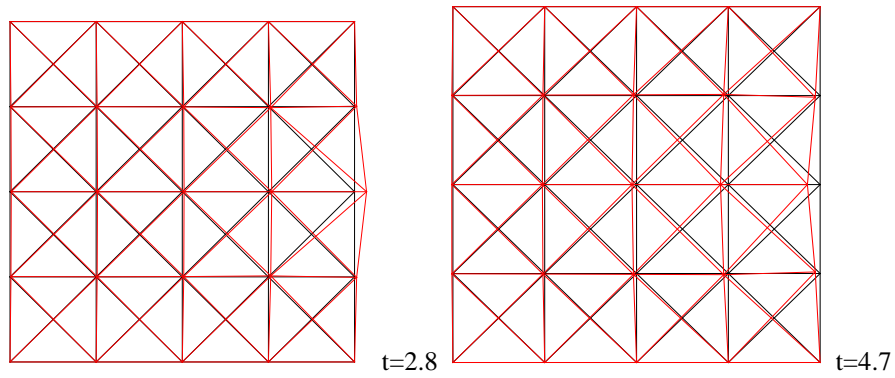


Fig. 21(b) Maxwell structure models in times $t = 2.8, 4.7, 10.5, 13, 14.4, 15$

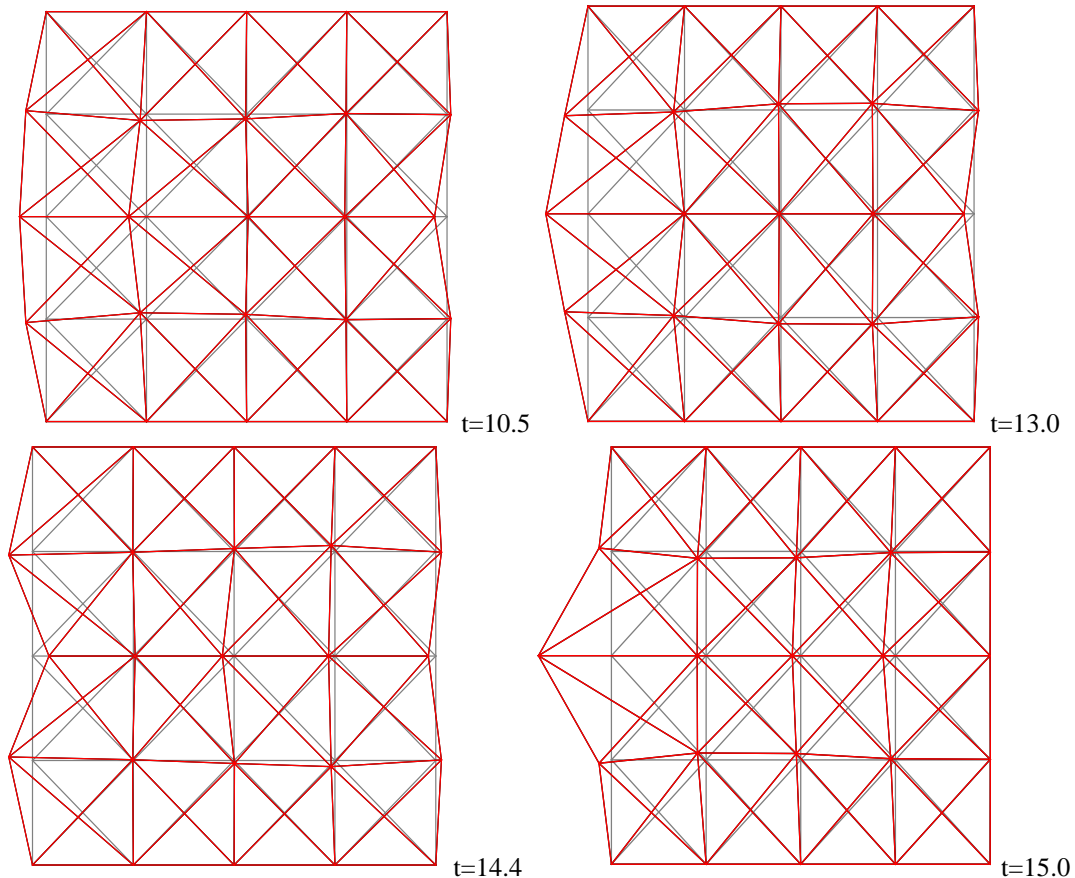


Fig. 21(b) Continued

From Fig. 21 (but even more from their animation), it is visible that in the Kelvin model a strain wave propagates through the material from one side of the sample to the other, causing finally material eruption at the exit; in the Maxwell model, a strain wave is reflecting from sides eventually superposing and causing eruption at the exit.

5.3 Comparison

Comparison of Kelvin based and Maxwell based models under impact and periodic loading reveals that for both models it is possible to obtain strain wave propagation and eruption of the material on the side opposite to the loading. Strain wave propagation looks realistic and mass and shape at the eruption are clearly dependent on the loading rate.

6. Conclusions

Some novel tools for the assessment of nonlinear material models are presented. They are applicable on models based on DAE and have been used for analysis of DAE based structure model with integrated standard nonlinear solid model. This paper can be considered as an extended

proof of concept for the application of a nonlinear version of the standard solid model in material response to dynamic loading. Numerical experiments have confirmed that:

- The model can realistically reproduce phenomena observed in experiments, including localization (and bifurcation).
- Addition of mass into the model is important for obtaining realistic response under dynamic loading (strain wave propagation).

The mass added to the structure model as a structural property is not sufficiently integrated with the material model and the response can be obtained only on the structure level, i.e., structural properties like eigenfrequencies and eigenvectors could be addressed.

The mass integrated into the material model can also address material properties like, i.e., strain wave propagation and fracture formation under different load rates. In this phase of the research, such a model has been based only on DAE; experimentation with some other types of solution procedures is planned in a later stage.

This model is certainly among the smallest models capable of realistic representation of strain wave propagation through the material sample.

In the future, Wolfram Mathematica model will be combined with Modelica programming environment, i.e., integrated with System Modeler in the hope of analyzing larger structures. In addition, future work will include some measure of nonlinearity based on the paper of Kerschen *et al.* (2006).

Acknowledgments

The Croatian Science Foundation Grant No. 9068 Multi-scale concrete model with parameter identification supported this work. The support is gratefully acknowledged.

References

- Do, X.N., Ibrahimbegovic, A. and Brancherie, D. (2015a), “Combined hardening and localized failure with softening plasticity in dynamics”, *Coupled Syst. Mech.*, **4**(2), 115-136.
- Do, X.N., Ibrahimbegovic, A. and Brancherie, D. (2015b), “Localized failure in damage dynamics”, *Coupled Syst. Mech.*, **4**(3), 211-235.
- Ermentrout, B. (2002), *Simulating, Analyzing, and Animating Dynamical Systems: A Guide to XPPAUT for Researchers and Students*, SIAM.
- Holger, K. and Thomas, S. (2003), *Nonlinear Time Series Analysis*, Cambridge University Press.
- <http://reference.wolfram.com/language> (2017), *Numerical Solution of Differential-Algebraic Equations*, Wolfram.
- <http://www.math.pitt.edu/~bard/xpp/xpp.html> (2016), *XPPAUT 8.0*, University of Pittsburgh.
- Ibrahimbegovic, A. (2009), *Nonlinear Solid Mechanics*, Springer
- Kantz, H. and Schreiber, T. (2003), *Nonlinear Time Series Analysis*, Cambridge University Press.
- Keivani, A., Shooshtari, A. and Sani, A.A. (2014), “Forced vibration analysis of a dam-reservoir interaction problem in frequency domain”, *Coupled Syst. Mech.*, **3**(4), 385-403.
- Kerschen, G., Worden, K., Vakakis, A.F. and Golinval, J.C. (2006), “Past, present and future of nonlinear system identification in structural dynamics”, *Mech. Syst. Sign. Proc.*, **20**, 505-592.
- Kožar, I. and Ožbolt, J. (2010), “Some aspects of load-rate sensitivity in visco-elastic microplane material model”, *Comput. Concrete*, **7**, 331-346.
- Kožar, I., Ožbolt, J. and Pecak, T. (2012), “Load-rate sensitivity in 1D non-linear viscoelastic model”, *Key*

Eng. Mater., **488-489**, 731-734.

Kun, F., Raischel, F., Hidalgo, R.C. and Herrmann, H.J. (2007), "Extensions of fiber bundle models", *Lect. Note. Phys.*, **705**, 57-92.

Liu, B. and Tang, S. (2016), "Heat jet approach for finite temperature atomic simulations of two-dimensional square lattice", *Coupled Syst. Mech.*, **5**(4), 371-393.

Marenić, E. and Ibrahimbegovic, A. (2015), "Homogenized elastic properties of graphene for moderate deformations", *Coupled Syst. Mech.*, **4**(2), 137-155.

Simo, J.C. and Hughes, T.J.R. (1998), *Computational Inelasticity*, Springer.

Toh, W., Ding, Z., Ng, T.Y. and Liu, Z. (2016), "Light intensity controlled wrinkling patterns in photo-thermal sensitive hydrogels", *Coupled Syst. Mech.*, **5**(4), 315-327.

Van, M. and Jan, G.M. (2013), *Concrete Fracture a Multiscale Approach*, CRC Press Taylor & Francis.

Ziaolhagh, S.H., Goudarzi, M. and Sani, A.A. (2016), "Free vibration analysis of gravity dam-reservoir system utilizing 21 node-33 Gauss point triangular elements", *Coupled Syst. Mech.*, **5**(1), 59-86.

AI